
3. Microemulsions

This chapter is devoted to another important property of surfactants, that of stabilization of water-oil films and formation of microemulsions. These are a special kind of colloidal dispersion that have attracted a great deal of attention because of their ability to solubilise otherwise insoluble materials. Industrial applications of microemulsions have escalated in the last 40 years following an increased understanding of formation, stability and the role of surfactant molecular architecture. This chapter reviews main theoretical features relevant to the present work and some common techniques used to characterize microemulsion phases.

3.1 MICROEMULSIONS: DEFINITION AND HISTORY

One of the best definitions of microemulsions is from Danielsson and Lindman [1] "*a microemulsion is a system of water, oil and an amphiphile which is a single optically isotropic and thermodynamically stable liquid solution*". In some respects, microemulsions can be considered as small-scale versions of emulsions, i.e., droplet type dispersions either of oil-in-water (o/w) or of water-in-oil (w/o), with a size range in the order of 5–50 nm in drop radius. Such a description, however, lacks precision since there are significant differences between microemulsions and ordinary emulsions (or macroemulsions). In particular, in emulsions the average drop size grows continuously with time so that phase separation ultimately occurs under gravitational force, i.e., they are thermodynamically unstable and their formation requires input of work. The drops of the dispersed phase are

generally large ($> 0.1 \mu\text{m}$) so that they often take on a milky, rather than a translucent appearance. For microemulsions, once the conditions are right, spontaneous formation occurs. As for simple aqueous systems, microemulsion formation is dependent on surfactant type and structure. If the surfactant is ionic and contains a single hydrocarbon chain (e.g., sodium dodecylsulphate, SDS) microemulsions are only formed if a co-surfactant (e.g., a medium size aliphatic alcohol) and/or electrolyte (e.g., 0.2 M NaCl) are also present. With double chain ionics (e.g., Aerosol-OT) and some non-ionic surfactants a co-surfactant is not necessary. This results from one of the most fundamental properties of microemulsions, that is, an ultra-low interfacial tension between the oil and water phases, $\gamma_{o/w}$. The main role of the surfactant is to reduce $\gamma_{o/w}$ sufficiently – i.e., lowering the energy required to increase the surface area – so that spontaneous dispersion of water or oil droplets occurs and the system is thermodynamically stable. As described in Section 3.2.1 ultra-low tensions are crucial for the formation of microemulsions and depend on system composition.

Microemulsions were not really recognized until the work of Hoar and Schulman in 1943, who reported a spontaneous emulsion of water and oil on addition of a strong surface-active agent [2]. The term “microemulsion” was first used even later by Schulman *et al.* [3] in 1959 to describe a multiphase system consisting of water, oil, surfactant and alcohol, which forms a transparent solution. There has been much debate about the word “microemulsion” to describe such systems [4]. Although not systematically used today, some prefer the names “micellar emulsion” [5] or “swollen micelles” [6]. Microemulsions were probably discovered well before the studies of Schulmann: Australian housewives have used since the beginning of last century water/eucalyptus oil/soap flake/white spirit mixtures to wash wool, and the first commercial microemulsions were probably the liquid waxes discovered by Rodawald in 1928. Interest in microemulsions really stepped up in the late 1970's and early 1980's when it was recognized that such systems could improve oil recovery and when oil prices reached levels where tertiary recovery methods became profit earning [7]. Nowadays this is no longer the case, but

other microemulsion applications were discovered, e.g., catalysis, preparation of submicron particles, solar energy conversion, liquid–liquid extraction (mineral, proteins, etc.). Together with classical applications in detergency and lubrication, the field remains sufficiently important to continue to attract a number of scientists. From the fundamental research point of view, a great deal of progress has been made in the last 20 years in understanding microemulsion properties. In particular, interfacial film stability and microemulsion structures can now be characterized in detail owing to the development of new and powerful techniques such as small-angle neutron scattering (SANS, as described in Chapter 4). The following sections deal with fundamental microemulsion properties, i.e., formation and stability, surfactant films, classification and phase behaviour.

3.2 THEORY OF FORMATION AND STABILITY

3.2.1 Interfacial tension in microemulsions

A simple picture for describing microemulsion formation is to consider a subdivision of the dispersed phase into very small droplets. Then the configurational entropy change, ΔS_{conf} , can be approximately expressed as [8]:

$$\Delta S_{\text{conf}} = -nk_{\text{B}}[\ln \phi + \{(1 - \phi)/\phi\} \ln(1 - \phi)] \quad (3.2.1)$$

where n is the number of droplets of dispersed phase, k_{B} is the Boltzmann constant and ϕ is the dispersed phase volume fraction. The associated free energy change can be expressed as a sum of the free energy for creating new area of interface, $\Delta A\gamma_{12}$, and configurational entropy in the form [9]:

$$\Delta G_{\text{form}} = \Delta A\gamma_{12} - T\Delta S_{\text{conf}} \quad (3.2.2)$$

where ΔA is the change in interfacial area A (equal to $4\pi r^2$ per droplet of radius r) and γ_{12} is the interfacial tension between phases 1 and 2 (e.g., oil and water) at temperature T (Kelvin). Substituting Eq. 3.2.1 into 3.2.2 gives an expression for obtaining the maximum interfacial tension between phases 1 and 2. On dispersion, the droplet number increases and ΔS_{conf} is positive. If the surfactant can reduce the interfacial tension to a sufficiently low value, the energy term in Eq. 3.2.2 ($\Delta A\gamma_{12}$) will be relatively small and positive, thus allowing a negative (and hence favourable) free energy change, that is, spontaneous microemulsification.

In surfactant-free oil–water systems, $\gamma_{o/w}$ is of the order of 50 mN m^{-1} , and during microemulsion formation the increase in interfacial area, ΔA , is very large, typically a factor of 10^4 to 10^5 . Therefore in the absence of surfactant, the second term in Eq. 3.2.2 is of the order of $1000 k_B T$, and in order to fulfill the condition $\Delta A\gamma_{12} \leq T\Delta S_{\text{conf}}$, the interfacial tension should be very low (approximately 0.01 mN m^{-1}). Some surfactants (double chain ionics [10, 11] and some non-ionics [12]) can produce extremely low interfacial tensions – typically 10^{-2} to $10^{-4} \text{ mN m}^{-1}$ – but in most cases, such low values cannot be achieved by a single surfactant since the CMC is reached before a low value of $\gamma_{o/w}$ is attained. An effective way to further decrease $\gamma_{o/w}$ is to include a second surface-active species (either a surfactant or medium-chain alcohol), that is a co-surfactant. This can be understood in terms of the Gibbs equation extended to multicomponent systems [13]. It relates the interfacial tension to the surfactant film composition and the chemical potential, μ , of each component in the system, i.e.,

$$d\gamma_{o/w} = -\sum_i (\Gamma_i d\mu_i) \approx -\sum_i (\Gamma_i RT d \ln C_i) \quad (3.2.3)$$

where C_i is the molar concentration of component i in the mixture, and Γ_i the surface excess (mol m^{-2}). Assuming that surfactants and co-surfactants, with concentration C_s and C_{co} respectively, are the only adsorbed components (i.e., $\Gamma_{\text{water}} = \Gamma_{\text{oil}} = 0$), Eq. 3.2.3 becomes:

$$d\gamma_{o/w} = -\Gamma_s RT d \ln C_s - \Gamma_{co} RT d \ln C_{co} \quad (3.2.4)$$

Integration of Eq. 3.2.4 gives:

$$\gamma_{o/w} = \gamma_{o/w}^\circ - \int_0^{C_s} \Gamma_s RT d \ln C_s - \int_0^{C_{co}} \Gamma_{co} RT d \ln C_{co} \quad (3.2.5)$$

Eq. 3.2.5 shows that $\gamma_{o/w}^\circ$ is lowered by two terms, both from the surfactant and co-surfactant (of surface excesses Γ_s and Γ_{co} respectively) so their effects are additive. It should be mentioned, however, that the two molecules should be adsorbed simultaneously and should not interact with each other (otherwise they lower their respective activities), i.e., are of completely different chemical nature, so that mixed micellisation does not occur.

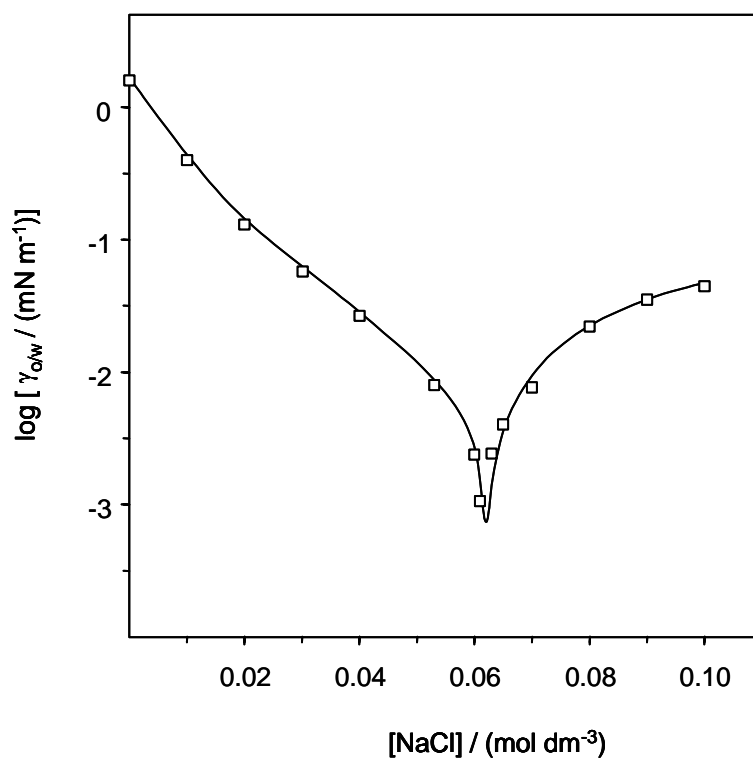
Figure 3.1 shows typical low interfacial tensions found in microemulsions, in this case spanning ~ 1 to 10^{-3} mN m⁻¹. The effect of salt concentration is consistent with changes in the phase behaviour, which are discussed in more detail in Section 3.3 and Figure 3.2 below.

3.2.2 Kinetic instability

Internal contents of the microemulsion droplets are known to exchange, typically on the millisecond time scale [16, 17]. They diffuse and undergo collisions. If collisions are sufficiently violent, then the surfactant film may rupture thereby facilitating droplet exchange, that is the droplets are kinetically unstable. However, if one disperses emulsions sufficiently small droplets (< 500 Å), the tendency to coalesce will be counteracted by an energy barrier. Then the system will remain dispersed and transparent for a long period of time (months) [18]. Such an emulsion is said to be kinetically stable [19]. The mechanism of droplet coalescence has been reported for AOT w/o microemulsions [16]; the droplet exchange process was characterized by a second order rate constant k_{ex} , which is believed to be activation controlled

(hence the activation energy, E_a , barrier to fusion) and not purely diffusion controlled. Other studies [20] have shown that the dynamic aspects of microemulsions are affected by the flexibility of the interfacial film, that is film rigidity (see Section 3.3.2), through a significant contribution to the energy barrier. Under the same experimental conditions, different microemulsion systems can have different k_{ex} values [16]: for AOT w/o system at room temperature, k_{ex} is in the range 10^6 – 10^9 $\text{dm}^3 \text{mol}^{-1} \text{s}^{-1}$, and for non-ionics $C_{12}E_6$, 10^8 – 10^9 $\text{dm}^3 \text{mol}^{-1} \text{s}^{-1}$ [16, 17, 20]. In any case, an equilibrium droplet shape and size is always maintained and this can be studied by different techniques [20].

Figure 3.1 Oil-water interfacial tension between *n*-heptane and aqueous NaCl solutions as a function of salt concentration in the presence of AOT surfactant. The values were determined by spinning drop tensiometry. The AOT surfactant concentration is $0.050 \text{ mol dm}^{-3}$, temperature 25°C .



3.3 PHYSICOCHEMICAL PROPERTIES

This section gives an overview of the main parameters characterizing microemulsions. References will be made to related behaviour for planar interfaces presented in Chapter 2.

3.3.1 Predicting microemulsion type

A well-known classification of microemulsions is that of Winsor [21] who identified four general types of phase equilibria:

- Type I: the surfactant is preferentially soluble in water and oil-in-water (o/w) microemulsions form (Winsor I). The surfactant-rich water phase coexists with the oil phase where surfactant is only present as monomers at small concentration.
- Type II: the surfactant is mainly in the oil phase and water-in-oil (w/o) microemulsions form. The surfactant-rich oil phase coexists with the surfactant-poor aqueous phase (Winsor II).
- Type III: a three-phase system where a surfactant-rich middle-phase coexists with both excess water and oil surfactant-poor phases (Winsor III or middle-phase microemulsion).
- Type IV: a single-phase (isotropic) micellar solution, that forms upon addition of a sufficient quantity of amphiphile (surfactant plus alcohol).

Depending on surfactant type and sample environment, types I, II, III or IV form preferentially, the dominant type being related to the molecular arrangement at the interface (see below). As illustrated in Figure 3.2, phase transitions are brought about by increasing either electrolyte concentration (in the case of ionic surfactants) or temperature (for non-ionics). Table 3.1 summarizes the qualitative changes in phase behaviour of anionic surfactants when formulation variables are modified [22].

Various investigators have focused on interactions in an adsorbed interfacial film to explain the direction and extent of interfacial curvature. The first concept was that of Bancroft [23] and Clowes [24] who considered the adsorbed film in emulsion systems to be duplex in nature, with an inner and an outer interfacial tension acting independently [25]. The interface would then curve such that the inner surface was one of higher tension. Bancroft's rule was stated as *"that phase will be external in which the emulsifier is most soluble"*; i.e., oil-soluble emulsifiers will form w/o emulsions and water-soluble emulsifiers o/w emulsions. This qualitative concept was largely extended and several parameters have been proposed to quantify the nature of the surfactant film. They are briefly presented in this section. Further details concerning these microemulsion types and their location in the phase diagram will be given in Section 3.3.3.

The R-ratio

The R-ratio was first proposed by Winsor [21] to account for the influence of amphiphiles and solvents on interfacial curvature. The primary concept is to relate the energies of interaction between the amphiphile layer and the oil and water regions. Therefore, this R-ratio compares the tendency for an amphiphile to disperse into oil, to its tendency to dissolve in water. If one phase is favoured, the interfacial region tends to take on a definite curvature. A brief description of the concept is given below, and a full account can be found elsewhere [26].

In micellar or microemulsion solutions, three distinct (single or multicomponent) regions can be recognized: an aqueous region, W, an oil or organic region, O, and an amphiphilic region, C. As shown in Figure 3.3, it is useful to consider the interfacial zone as having a definite composition, separating essentially bulk-phase water from bulk-phase oil. In this simple picture, the interfacial zone has a finite thickness, and will contain, in addition to surfactant molecules, some oil and water.

Figure 3.2 Winsor classification and phase sequence of microemulsions encountered as temperature or salinity is scanned for non-ionic and ionic surfactant respectively. Most of the surfactant resides in the shaded area. In the three-phase system the middle-phase microemulsion (M) is in equilibrium with both excess oil (O) and water (W).

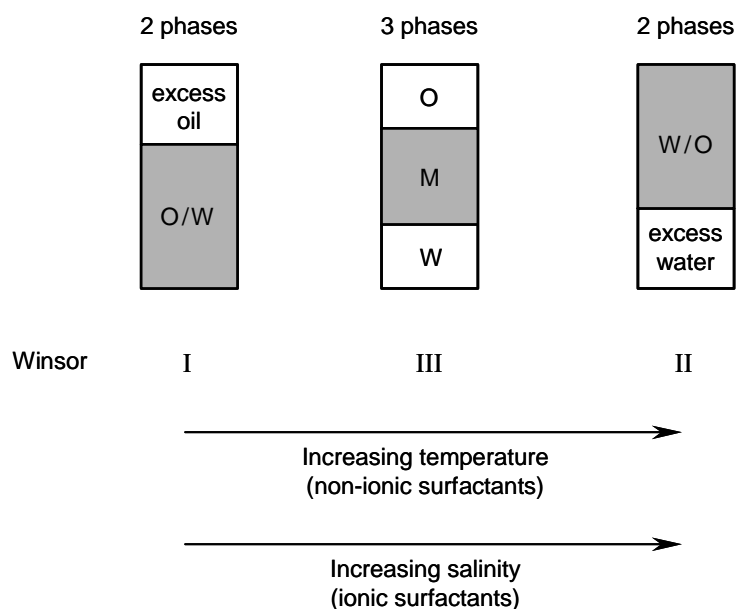
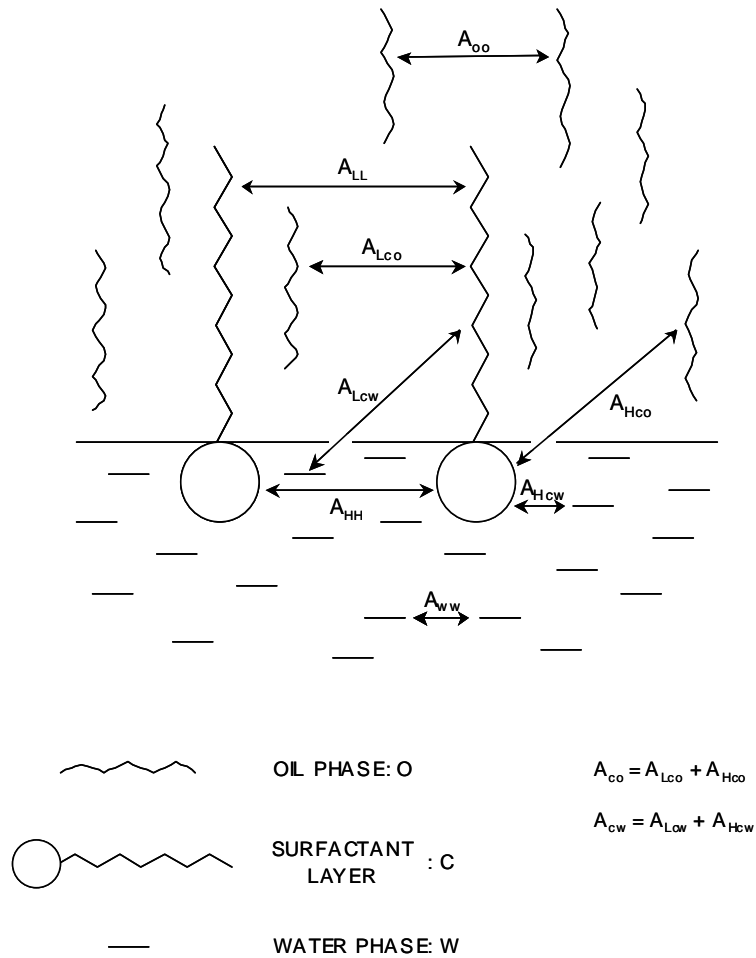


Table 3.1 Qualitative effect of several variables on the observed phase behaviour of anionic surfactants. After Bellocq *et al.* [22]

Scanned variables (increase)	Ternary diagram transition
Salinity	I \times III \times II
Oil: Alkane carbon number	II \times III \times I
Alcohol: low M.W. ^a	I \times III \times II
high M.W. ^b	I \times III \times II
Surfactant: lipophilic chain length	I \times III \times II
Temperature	II \times III \times I

Figure 3.3 Interaction energies in the interfacial region of an oil-surfactant-water system.



Cohesive interaction energies therefore exist within the C layer, and these determine interfacial film stability. They are depicted schematically in Figure 3.3: the cohesive energy between molecules x and y is defined as A_{xy} , and is positive whenever interaction between molecules is attractive. A_{xy} is depicted as the cohesive energy per unit area between surfactant, oil and water molecules residing in the anisotropic interfacial C layer. For surfactant–oil and surfactant–water interactions A_{xy} can be considered to be composed of two additive contributions:

$$A_{xy} = A_{Lxy} + A_{Hxy} \quad (3.3.1)$$

where A_{Lxy} quantifies interaction between nonpolar portions of the two molecules (typically London dispersion forces) and A_{Hxy} represents polar interactions, especially hydrogen bonding or Colombic interactions. Thus, for surfactant–oil and surfactant–water interactions, cohesive energies to be considered are:

- $A_{co} = A_{Lco} + A_{Hco}$ (3.3.2)

- $A_{cw} = A_{Lcw} + A_{Hcw}$ (3.3.3)

A_{Hco} and A_{Lcw} are generally very small values and can be ignored.

Other cohesive energies are those arising from the following interactions:

- water–water, A_{ww}
- oil–oil, A_{oo}
- hydrophobic–hydrophobic parts (L) of surfactant molecules, A_{LL}
- hydrophilic–hydrophilic parts (H) of surfactant molecules, A_{HH}

The cohesive energy A_{co} evidently promotes miscibility of the surfactant molecules with the oil region, and A_{cw} with water. On the other hand, A_{oo} and A_{LL} oppose miscibility with oil, while A_{ww} and A_{HH} oppose miscibility with water. Therefore, interfacial stability is ensured if the difference in solvent interactions in C with oil and water bulk phases is sufficiently small. Too large a difference, i.e., too strong affinity of C for one phase or the other, would drive to a phase separation.

Winsor expressed qualitatively this variation in dispersing tendency by:

$$R = \frac{A_{co}}{A_{cw}} \quad (3.3.4)$$

To account for the structure of the oil, and the interactions between surfactant molecules, an extended version of the original R-ratio was proposed [26]:

$$R = \frac{(A_{co} - A_{oo} - A_{ll})}{(A_{cw} - A_{ww} - A_{hh})} \quad (3.3.5)$$

As mentioned before, in many cases, A_{Hco} and A_{Lcw} are negligible, so A_{co} and A_{cw} can be approximated respectively to A_{Lco} and A_{Hcw} .

In brief, Winsor's primary concept is that this R-ratio of cohesive energies, stemming from interaction of the interfacial layer with oil, divided by energies resulting from interactions with water, determines the preferred interfacial curvature. Thus, if $R > 1$, the interface tends to increase its area of contact with oil while decreasing its area of contact with water. Thus oil tends to become the continuous phase and the corresponding characteristic system is type II (Winsor II). Similarly, a balanced interfacial layer is represented by $R = 1$.

Packing parameter and microemulsion structures

Changes in film curvature and microemulsion type can be addressed quantitatively in terms of geometric requirements. This concept was introduced by Israelachvili *et al.* [27] and is widely used to relate surfactant molecular structure to interfacial topology. As described in Section 2.3.3, the preferred curvature is governed by relative areas of the head group, a_o , and the tail group, v/l_c (see Figure 2.6 for the possible aggregate structures). In terms of microemulsion type,

- if $a_o > v/l_c$, then an oil-in-water microemulsion forms,
- if $a_o < v/l_c$, then a water-in-oil microemulsion forms,
- if $a_o \approx v/l_c$, then a middle-phase microemulsion is the preferred structure.

Hydrophilic–Lipophilic Balance (HLB)

Another concept relating molecular structure to interfacial packing and film curvature is HLB, the hydrophilic–lipophilic balance. It is generally

expressed as an empirical equation based on the relative proportions of hydrophobic and hydrophilic groups within the molecule. The concept was first introduced by Griffin [28] who characterized a number of surfactants, and derived an empirical equation for non-ionic alkyl polyglycol ethers (C_iE_j) based on the surfactant chemical composition [29]:

$$\text{HLB} = (\text{E}_j \text{ wt\%} + \text{OH wt\%})/5 \quad (3.3.6)$$

where E_j wt% and OH wt% are the weight percent of ethylene oxide and hydroxide groups respectively.

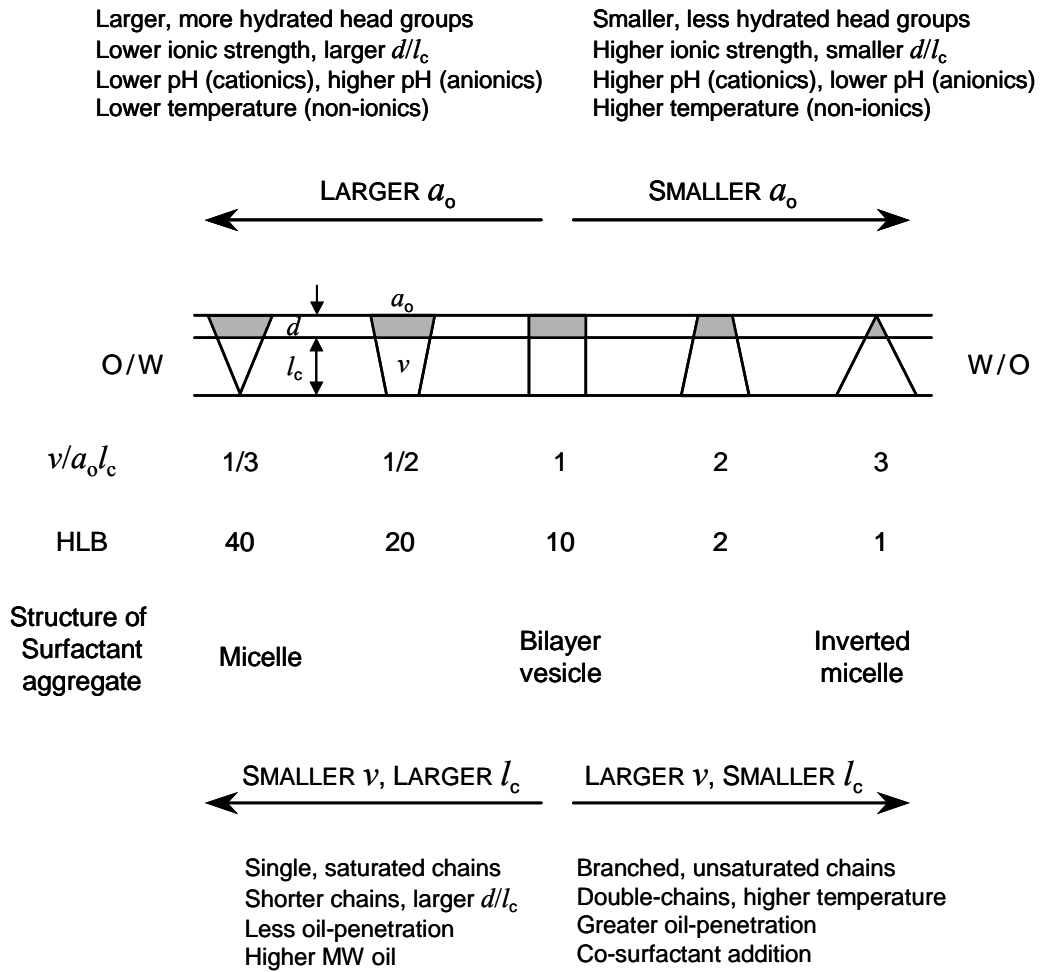
Davies *et al.* [30] proposed a more general empirical equation that associates a constant to the different hydrophilic and hydrophobic groups:

$$\text{HLB} = [(n_H \times H) - (n_L \times L)] + 7 \quad (3.3.7)$$

where H and L are constants assigned to hydrophilic and hydrophobic groups respectively, and n_H and n_L the number of these groups per surfactant molecule.

For bicontinuous structures, i.e., zero curvature, it was shown that $\text{HLB} \approx 10$ [31]. Then w/o microemulsions form when $\text{HLB} < 10$, and o/w microemulsion when $\text{HLB} > 10$. HLB and packing parameter describe the same basic concept, though the latter is more suitable for microemulsions. The influence of surfactant geometry and system conditions on HLB numbers and packing parameter is illustrated in Figure 3.4.

Figure 3.4 Effect of molecular geometry and system conditions on the packing parameter and HLB number (after Israelachvili [31]).



Phase Inversion Temperature (PIT)

Non-ionic surfactants form water–oil microemulsions (and emulsions) with a high temperature sensitivity. In particular, there is a specific phase inversion temperature (PIT) and the film curvature changes from positive to negative. This critical point was defined by Shinoda *et al.* [32]:

- if $T < \text{PIT}$, an oil-in-water microemulsion forms (Winsor I),
- if $T > \text{PIT}$, a water-in-oil microemulsion forms (Winsor II),
- at $T = \text{PIT}$, a middle-phase microemulsion exists (Winsor III) with a spontaneous curvature equal to zero, and a HLB number (Eq. 3.3.6) approximately equal to 10.

The HLB number and PIT are therefore connected; hence the term HLB temperature is sometimes employed [33].

3.3.2 Surfactant film properties

an alternative, more physically realistic, approach is to consider mechanical properties of a surfactant film at an oil–water interface. This film can be characterized by three phenomenological constants: tension, bending rigidity, and spontaneous curvature. Their relative importance depends on the constraints felt by the film. It is important to understand how these parameters relate to interfacial stability since surfactant films determine the static and dynamic properties of microemulsions (and emulsions). These include phase behaviour and stability, structure, and solubilisation capacity.

Ultra-low interfacial tension

Interfacial (or surface) tensions, γ , were defined in Chapter 2 for planar surfaces, and the same principle applies for curved liquid–liquid interfaces, i.e., it corresponds to the work required to increase interfacial area by unit amount. As mentioned in Section 3.2.1, microemulsion formation is accompanied by ultra-low interfacial oil–water tensions, $\gamma_{o/w}$, typically 10^{-2} to 10^{-4} mN m⁻¹. They are affected by the presence of a co-surfactant, as well as electrolyte and/or temperature, pressure, and oil chain length. Several studies have been reported on the effect of such variables on $\gamma_{o/w}$. In particular, Aveyard and coworkers performed several systematic interfacial tension measurements on both ionics [34, 35] and non-ionics [36], varying oil chain length, temperature, and electrolyte content. For example, in the system water–AOT–*n*-heptane, at constant surfactant concentration (above its CMC), a plot of $\gamma_{o/w}$ as a function of electrolyte (NaCl) concentration shows a deep minimum that corresponds to the Winsor phase inversion; i.e., upon addition of NaCl, $\gamma_{o/w}$ decreases to a minimum critical value (Winsor III structure), then increases to a limiting value close to 0.2–0.3 mN m⁻¹ (Winsor II region). At constant electrolyte concentration, varying temperature [34], oil chain length and co-surfactant

content [35] have a similar effect. With non-ionics, a similar tension curve and phase inversion are observed, but on increasing temperature [36]. In addition, when increasing surfactant chain length, the interfacial tension curves shift to higher temperatures and the minimum in $\gamma_{o/w}$ decreases [37]. Ultra-low interfacial tensions cannot be measured with standard techniques such as Du Nouy Ring, Wilhelmy plate, or drop volume (DVT). Appropriate techniques for this low tension range are spinning drop tensiometry (SDT) and surface light scattering [38].

Spontaneous curvature

Spontaneous (or natural or preferred) curvature C_0 is defined as the curvature formed by a surfactant film when a system consists of equal amounts of water and oil. Then, there is no constraint on the film, which is free to adopt the lowest free energy state. Whenever one phase is predominant, there is a deviation from C_0 . In principle, every point on a surface possesses two principal radii of curvature, R_1 and R_2 and their associated principal curvatures are $C_1 = 1/R_1$ and $C_2 = 1/R_2$. Mean and Gaussian curvatures are used to define the bending of surfaces. They are defined as follows [39]:

$$\text{Mean curvature: } C = \frac{1}{2} (1/R_1 + 1/R_2)$$

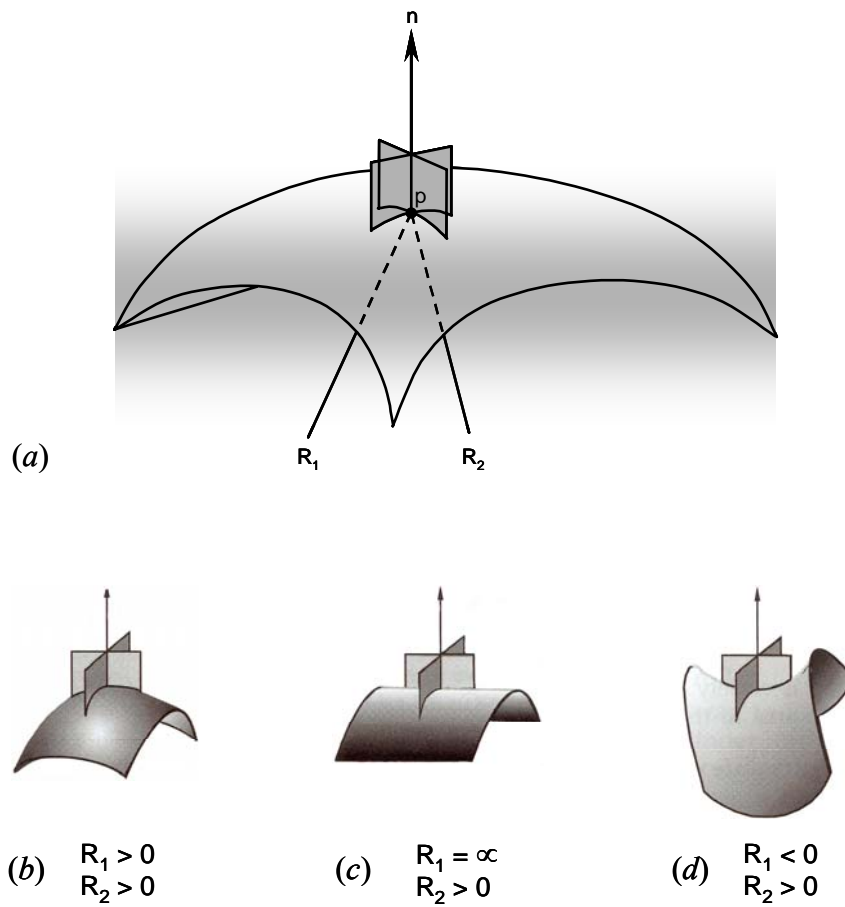
$$\text{Gaussian curvature: } \kappa = 1/R_1 \times 1/R_2$$

C_1 and C_2 are determined as follows: every point on the surface of the surfactant film has two principal radii of curvature, R_1 and R_2 as shown in Figure 3.5. If a circle is placed tangentially to a point p on the surface and if the circle radius is chosen so that its second derivative at the contact point equals that of the surface in the direction of the tangent (of normal vector, n), then the radius of the circle is a radius of curvature of the surface. The curvature of the surface is described by two such circles chosen in orthogonal (principal) directions as shown in Figure 3.5(a).

For a sphere, R_1 and R_2 are equal and positive (Figure 3.5(b)). For a cylinder R_2 is indefinite (Figure 3.5(c)) and for a plane, both R_1 and R_2 are indefinite. In the special case of a saddle, $R_1 = -R_2$, i.e., at every point the surface is both concave and convex (Figure 3.5(d)). Both a plane and saddle have the property of zero mean curvature.

The curvature C_o depends both on the composition of the phases it separates and on surfactant type. One argument applied to the apolar side of the interface is that oil can penetrate to some extent between the surfactant hydrocarbon tails. The more extensive the penetration, the more curvature is imposed toward the polar side. This results in a decrease of C_o since, by convention, positive curvature is toward oil (and negative toward water). The longer the oil chains, the less they penetrate the surfactant film and the smaller the effect on C_o . Recently, Eastoe *et al.* have studied the extent of solvent penetration in microemulsions stabilized by di-chained surfactants, using SANS and selective deuteration. Results suggested that oil penetration is a subtle effect, which depends on the chemical structures of both surfactant and oil. In particular, unequal surfactant chain length [40-43] or presence of C = C bonds [44] result in a more disordered surfactant/oil interface, thereby providing a region of enhanced oil mixing. For symmetric di-chained surfactants (e.g., DDAB and AOT), however, no evidence for oil mixing was found [42]. The effect of alkane structure, and molecular volume on the oil penetration was also investigated with n-heptane, and cyclohexane. The results indicate that heptane is essentially absent from the layers, but the more compact cyclohexane has a greater penetrating effect [43].

Figure 3.5 Principal curvatures of different surfaces. (a) Intersection of the surfactant film surface with planes containing the normal vector (n) to the surface at the point p . (b) convex curvature, (c) cylindrical curvature, (d) saddle-shaped curvature. After Hyde *et al.* [39].



Surfactant type, and nature of the polar head group, also influences C_o through different interactions with the polar (aqueous) phase:

- For ionic surfactants electrolyte content and temperature affect the spontaneous curvature in opposite ways. An increase in salt concentration screens electrostatic head group repulsions – i.e., decreases head group area – so the film curves more easily toward water, leading to a decrease in C_o . Raising temperature has two effects: (1) an increase in electrostatic repulsions between head groups due to higher counterion dissociation, so C_o increases; (2) more gauche conformations are induced in the surfactant chains, which become more coiled, resulting in a decrease in C_o . Therefore the combined effects of temperature on the apolar chains and on electrostatic interactions are competitive. The electrostatic term is believed to be slightly dominant, so C_o increases weakly with increasing temperature.
- For non-ionic surfactants, unsurprisingly, electrolytes have very little effect on C_o , whereas temperature is a critical parameter due to the strong dependence of their solubility (in water or oil) on temperature. For surfactants of the C_iE_j type as temperature increases water becomes a less good solvent for the hydrophilic units and penetrates less into the surfactant layer. In addition, on the other side of the film, oil can penetrate further into the hydrocarbon chains, so that increasing temperature for this type of surfactant causes a strong decrease in C_o . This phenomenon explains the strong temperature effects on the phase equilibria of such surfactants as shown in Figure 2.8 (see Chapter 2).

Thus, by changing external parameters such as temperature, nature of the oil or electrolyte concentration, the spontaneous curvature can be tuned to the appropriate value, and so drive transitions between Winsor systems. Other factors affect C_o in a similar fashion; they include varying the polar head group,

type and valency of counterions, length and number of apolar chains, adding a co-surfactant, or mixing surfactants.

Film bending rigidity

Film rigidity is an important parameter associated with interfacial curvature. The concept of film bending energy was first introduced by Helfrich [45] and is now considered as an essential model for understanding microemulsion properties. It can be described by two elastic moduli [46] that measure the energy required to deform the interfacial film from a preferred mean curvature:

- the mean bending elasticity (or rigidity), K , associated with the mean curvature, that represents the energy required to bend unit area of surface by unit amount. K is positive, i.e., spontaneous curvature is favoured;
- the factor \bar{K} is associated with Gaussian curvature, and hence accounts for film topology. \bar{K} is negative for spherical structures or positive for bicontinuous cubic phases.

Theoretically, it is expected that bending moduli should depend on surfactant chain length [47], area per surfactant molecule in the film [48] and electrostatic head group interactions [49].

The film rigidity theory is based on the interfacial free energy associated with film curvature. The free energy, F , of a surfactant layer at a liquid interface may be given by the sum of an interfacial energy term, F_i , a bending energy term, F_b , and an entropic term, F_{ent} . For a droplet type structure this is written as [50]:

$$F = F_i + F_b + F_{\text{ent}} = \gamma A + \int \left[\frac{K}{2} (C_1 + C_2 - 2C_0)^2 + \bar{K} C_1 C_2 \right] dA + nk_B T f(\phi) \quad (3.3.8)$$

where γ is the interfacial tension, A is the total surface area of the film, K is the mean elastic bending modulus, \bar{K} is the Gaussian bending modulus, C_1 and C_2

are the two principal curvatures, C_0 the spontaneous curvature, n is the number of droplets, k_B is the Boltzmann constant, and $f(\phi)$ is a function accounting for the entropy of mixing of the microemulsion droplets, where ϕ is the droplet core volume fraction. For dilute systems where $\phi < 0.1$, it was shown that $f(\phi) = [\ln(\phi) - 1]$ [50]. Microemulsion formation is associated with ultra-low interfacial tension, γ so the γA term is small compared to F_b and F_{ent} and can be ignored as an approximation.

As mentioned previously, the curvatures C_1 , C_2 and C_0 can be expressed in terms of radii as $1/R_1$, $1/R_2$, and $1/R_0$ respectively. For spherical droplets, $R_1 = R_2 = R$, and the interfacial area is $A = n4\pi R^2$. Note that R and R_0 are core radii rather than droplet radii [50]. Solving Eq. 3.3.8 and dividing by area A , the total free energy, F , for spherical droplets (of radius R) is expressed as:

$$\frac{F}{A} = 2K \left(\frac{1}{R} - \frac{1}{R_0} \right)^2 + \frac{\bar{K}}{R^2} + \left[\frac{k_B T}{4\pi R^2} f(\phi) \right] \quad (3.3.9)$$

For systems where the solubilisation boundary is reached (WI or WII region), a microemulsion is in equilibrium with an excess phase of the solubilisate and the droplets have achieved their maximum size, i.e., the maximum core radius, R_{max}^{av} . Under this condition the minimization of the total free energy leads to a relation between the spontaneous radius, R_0 , and the elastic constants K and \bar{K} [51]:

$$\frac{R_{max}^{av}}{R_0} = \frac{2K + \bar{K}}{2K} + \frac{k_B T}{8\pi K} f(\phi) \quad (3.3.10)$$

A number of techniques have been used to determine K and \bar{K} separately, in particular, ellipsometry, X-ray reflectivity, and small-angle X-ray scattering (SAXS) techniques [52-54]. De Gennes and Taupin [55] have developed a model for bicontinuous microemulsions. For $C_0 = 0$ the layer is

supposed to be flat in the absence of thermal fluctuations. They introduced the term ξ_K , the persistence length of the surfactant layer that relates to K via:

$$\xi_K = a \exp(2\pi K / k_B T) \quad (3.3.11)$$

where a is a molecular length and ξ_K is the correlation length for the normals to the layer, i.e., the distance over which this layer remains flat in the presence of thermal fluctuations. ξ_K is extremely sensitive to the magnitude of K . When $K \gg k_B T$, ξ_K is macroscopic, i.e., the surfactant layer is flat over large distances and ordered structures such as lamellar phases may form. If K is reduced to $\sim k_B T$ then ξ_K is microscopic, ordered structures are unstable and disordered phases such as microemulsions may form. Experiments reveal that K is typically between $100 k_B T$ for condensed insoluble monolayers [56] and about $10 k_B T$ for lipid bilayers [57-59] but can decrease below $k_B T$ in microemulsion systems [60]. The role of \bar{K} is also important, however, there are few measurements of this quantity in the literature [e.g., 53, 61]. Its importance in determining the structure of surfactant–oil–water mixtures is still far from clear.

An alternative, more accessible, method to quantify film rigidities is to calculate the composite parameter $(2K + \bar{K})$ using tensiometry and SANS techniques. This parameter can be derived for droplet microemulsion at the solubilisation boundary, WI or WII system, by combining the radius of the droplet with interfacial tensions or droplet polydispersity. Two expressions can be derived from Eq. 3.3.9 and 3.3.10.

1. *Using the interfacial tension $\gamma_{o/w}$ (measured by SLS or SDT) and the maximum mean core radius R_{max}^{av} (measured by SANS see Chapter 4):*

$\gamma_{o/w}$ at the interface between microemulsion and excess phases at the solubilisation boundary can be expressed in terms of these elastic moduli and R_{max}^{av} [52]. Any new area created must be covered by a monolayer of surfactant, and so this energy may be calculated in the case of WI or WII systems since the surfactant monolayer is taken from around the curved

microemulsion droplets [56]. To do this it is necessary to unbend the surfactant film, introducing a contribution from K , of $2K/(R_{\max}^{\text{av}})^2$. The resulting change in the number of microemulsion droplets introduces an entropic contribution and a contribution due to the change in topology involving \bar{K} , of $\bar{K}/(R_{\max}^{\text{av}})^2$. So the interfacial tension between the microemulsion and excess phase is given by:

$$\gamma_{\text{o/w}} = \frac{2K + \bar{K}}{(R_{\max}^{\text{av}})^2} + \frac{k_B T}{4\pi(R_{\max}^{\text{av}})^2} f(\phi) \quad (3.3.11)$$

which gives for the bending moduli:

$$2K + \bar{K} = \gamma_{\text{o/w}} (R_{\max}^{\text{av}})^2 - \frac{k_B T}{4\pi} f(\phi) \quad (3.3.12)$$

2. *Using the Schultz polydispersity width $p = \sigma/R_{\max}^{\text{av}}$ obtained from SANS analysis (see Chapter 4):*

Droplet polydispersity relates to the bending moduli through thermal fluctuations of the microemulsion droplets. Safran [62] and Milner [63] described the thermal fluctuations by an expansion of the droplet deformation in terms of spherical harmonics. The principal contribution to these fluctuations was found to arise from the deformation mode $l = 0$ only [50]; and $l = 0$ deformations are fluctuations in droplet size, i.e., changes of the mean droplet radius and hence the droplet polydispersity. In the case of the two phase equilibria at maximum solubilisation (WI or WII), this polydispersity, p , may be expressed as a function of K and \bar{K} :

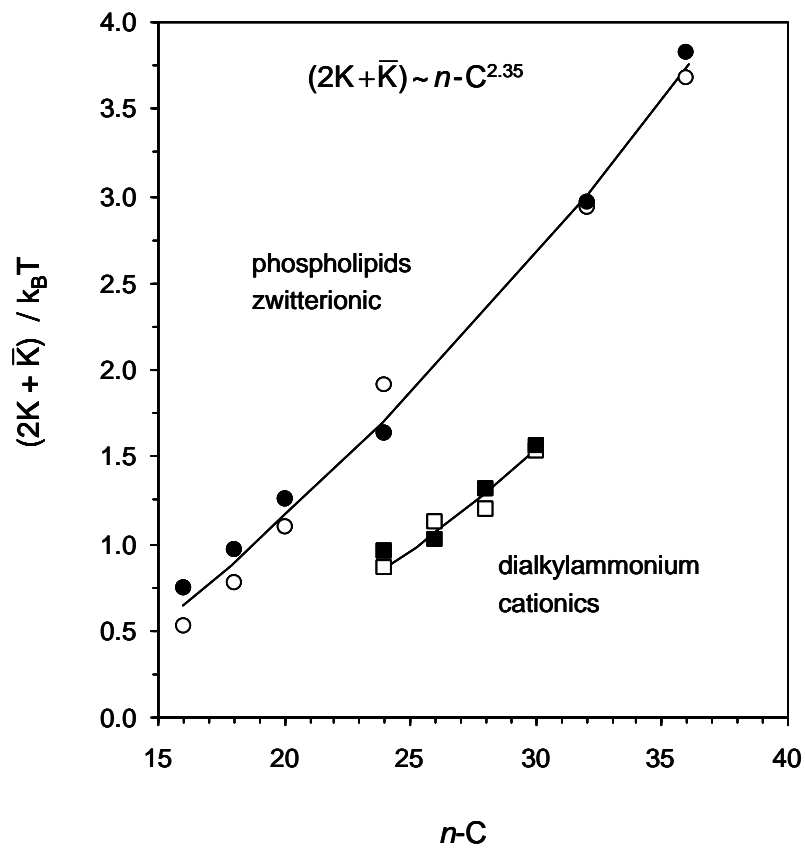
$$p^2 = \frac{u_o^2}{4\pi} = \frac{k_B T}{8\pi(2K + \bar{K}) + 2k_B T f(\phi)} \quad (3.3.13)$$

where u_o is the fluctuation amplitude for the $l = 0$ mode. This polydispersity is given by the SANS Schultz polydispersity parameter $\sigma/R_{\max}^{\text{av}}$ [64], and Eq. 3.3.13 can be written:

$$2K + \bar{K} = \frac{k_B T}{8\pi(\sigma/R_{\max}^{\text{av}})^2} - \frac{k_B T}{4\pi} f(\phi) \quad (3.3.14)$$

Therefore Eq. 3.3.12 and 3.3.14 give two accessible expressions for the sum $(2K + \bar{K})$ using data from SANS and tensiometry. This approach has been shown to work well with non-ionic films in WI systems [50, 65], and also cationic [64] and zwitterionic [66] layers in WII microemulsions. Figure 3.6 shows results for these latter two classes of system, as a function of surfactant alkyl carbon number n -C. The good agreement between equation 3.3.12 and 3.3.14 suggests they can be used with confidence. These values are in line with current statistical mechanical theories [48], which suggest that K should vary as n -C^{2.5} to n -C³, whereas there is only a small effect on \bar{K} .

Figure 3.6 Film rigidities ($2K + \bar{K}$) as a function of total alkyl carbon number n -C from Winsor II microemulsions. The lines are guides to the eye.



SANS $(2K + \bar{K}) = \frac{k_B T}{8\pi(\sigma/R_{\max}^{av})^2} - \frac{k_B T}{4\pi} f(\phi)$ ● ■

SANS & tensiometry $(2K + \bar{K}) = \gamma_{o/w} (R_{\max}^{av})^2 - \frac{k_B T}{4\pi} f(\phi)$ ○ □

3.3.3 Phase behaviour

Solubilisation and interfacial properties of microemulsions depend upon pressure, temperature and also on the nature and concentration of the components. The determination of phase stability diagrams (or phase maps), and location of the different structures formed within these water(salt)–oil–surfactant–alcohol systems in terms of variables are, therefore, very important. Several types of phase diagram can be identified depending on the number of variables involved. In using an adequate mode of representation, it is possible to describe not only the limits of existence of the single and multiphase regions, but also to characterize equilibria between phases (tie-lines, tie-triangles, critical points, etc.). Below is a brief description of ternary and binary phase maps, as well as the phase rule that dictates their construction.

Phase rule

The phase rule enables the identification of the number of variables (or degrees of freedom) depending on the system composition and conditions. It is generally written as [67]:

$$F = C - P + 2 \quad (3.3.15)$$

where F is the number of possible independent changes of state or degrees of freedom, C the number of independent chemical constituents, and P the number of phases present in the system. A system is called invariant, monovariant, bivariant, and so on, according to whether F is zero, 1, 2, and so on. For example, in the simplest case of a system composed of three components and two phases, F is univariant at a fixed temperature and pressure. This means that the mole or weight fraction of one component in one of the phases can be specified but all other compositions in both phases are fixed. In general, microemulsions contain at least three components: oil (O), water (W) and amphiphile (S), and as mentioned previously a co-surfactant (alcohol) and/or an electrolyte are usually added to tune the system stability. These can be considered as simple O–W–S systems: whenever a co-surfactant

is used, the ratio oil:alcohol is kept constant and it is assumed that the alcohol does not interact with any other component so that the mixture can be treated (to a first approximation) as a three-component system. At constant pressure, the composition–temperature phase behaviour can be presented in terms of a phase prism, as illustrated in Figure 3.7. However, the construction of such a phase map is rather complex and time consuming so it is often convenient to simplify the system by studying specific phase-cuts. The number of variables can be reduced either by keeping one term constant and/or by combining two or more variables. Then, ternary and binary phase diagrams are produced.

Ternary phase diagrams

At constant temperature and pressure, the ternary phase diagram of a simple three-component microemulsion is divided into two or four regions as shown in Figure 3.8. In each case, every composition point within the single-phase region above the demixing line corresponds to a microemulsion. Composition points below this line correspond to multiphase regions comprising in general microemulsions in equilibrium with either an aqueous or an organic phase or both, i.e., Winsor type systems (see Section 3.3.1).

Any system whose overall composition lies within the two-phase region (e.g., point *o* in Figures 3.8(a) and 3.8(c)) will exist as two phases whose compositions are represented by the ends of the “tie-line”, i.e., a segment formed by phases *m* and *n*. Therefore, every point on a particular tie-line has identical coexisting phases (*m* and *n*) but of different relative volumes. When the two conjugate phases have the same composition ($m = n$), this corresponds to the plait (or critical) point, *p*.

If three phases coexist (Figure 3.8(b)), i.e., corresponding to WIII, the system at constant temperature and pressure is, according to the phase rule, invariant. Then, there is a region of the ternary diagram that consists of three-phase systems having invariant compositions and whose boundaries are tie-lines in the adjacent two-phase regions that surround it. This region of three-phase invariant compositions is therefore triangular in form and called “tie-

triangle" [26]. Any overall composition, such as point q (Figure 3.8(b)) lying within the tie-triangle will divide into three phases having compositions corresponding to the vertices A, B, and C of the triangle. The compositions A, B, and C are invariant in the sense that varying the position q , the overall composition, throughout the triangle will result in variations in the amounts of the phases A, B, and C but not in their composition.

Figure 3.7 The phase prism, describing the phase behaviour of a ternary system at constant pressure.

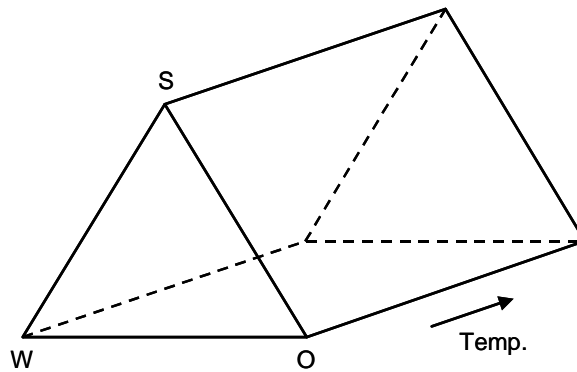
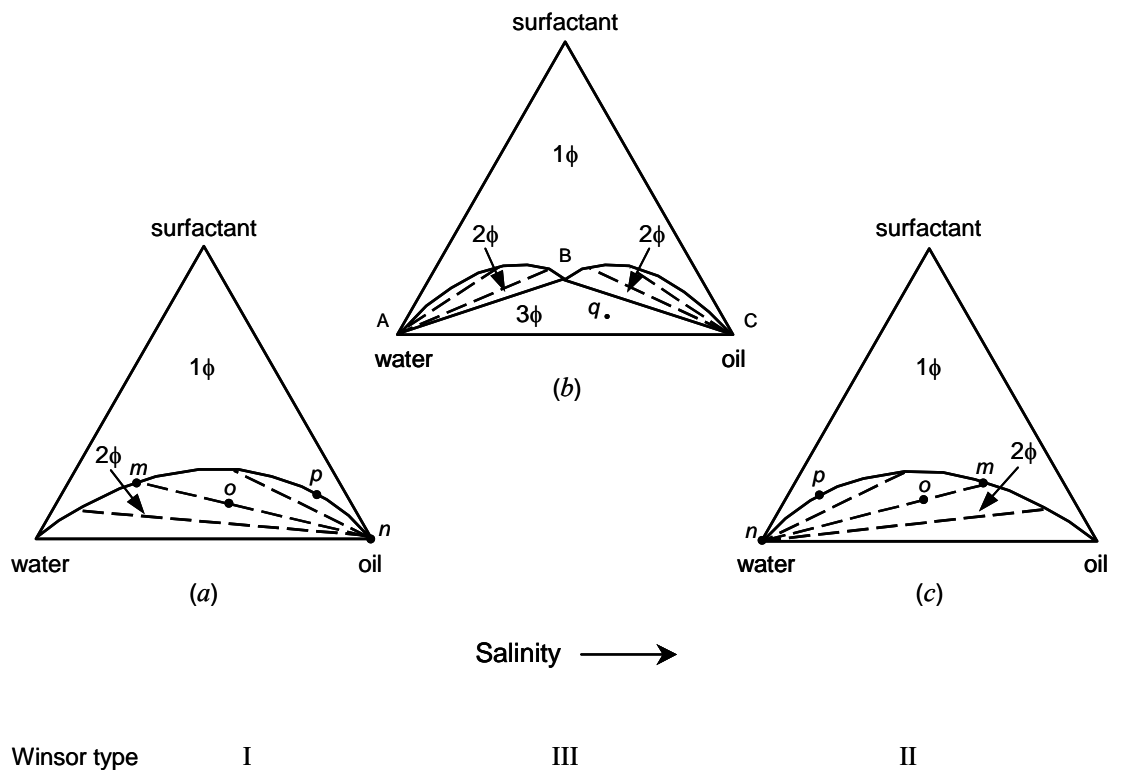


Figure 3.8 Ternary diagram representations of two- and three-phase regions formed by simple water–oil–surfactant systems at constant temperature and pressure. (a) Winsor I type, (b) Winsor II type, (c) Winsor III type systems.



Binary phase diagrams

As mentioned previously, ternary diagrams can be further simplified by fixing some parameters and/or combining two variables together (e.g., water and electrolyte into brine, or water and oil into water-to-oil ratio), i.e., reducing the degrees of freedom. Then, determining the phase diagram of such systems reduces to a study of a planar section through the phase prism. Examples of such pseudo-binary diagrams are given in Figures 3.9 to 3.11 for non-ionic and anionic surfactants.

Figure 3.9 shows the schematic phase diagram for a non-ionic surfactant–water–oil ternary system. Since temperature is a crucial variable in the case of non-ionics, the pseudo-binary diagram is represented by the planar section defined by $\phi_w = \phi_o$, where ϕ_w and ϕ_o are the volume fractions of water and oil respectively. Then, at constant pressure, defining the system in a single-phase region requires the identification of two independent variables ($F = 2$), i.e., temperature and surfactant concentration. The section shown in Figure 3.9(b) can be used to determine T_L and T_U , the lower and upper temperatures, respectively, of the phase equilibrium W+M+O (with M, the microemulsion phase), and the minimum amount of surfactant necessary to solubilise equal amounts of water and oil, denoted C_s^* [68]. The lower C_s^* the more efficient the surfactant. Figure 3.10 illustrates the determination of a second possible section for a non-ionic surfactant–water–oil ternary system: pressure and surfactant concentration are kept constant, leaving the two variables, temperature and water-to-oil ratio (ϕ_{w-o}). This diagram shows the various surfactant phases obtained as a function of temperature and water-to-oil ratio [68]. The third example (Figure 3.11) concerns an anionic surfactant, Aerosol-OT. In order to obtain $F = 2$ when defining the ternary W–O–S system in a single-phase region at constant pressure, the surfactant concentration parameter is fixed. Then, the two variables are temperature and w , the water-to-surfactant molar ratio defined as $w = [\text{water}] / [\text{surfactant}]$. w represents the number of water molecules solubilised per surfactant molecule, so that this phase diagram characterizes the surfactant efficiency, as a microemulsifier.

Figure 3.9 Binary phase behaviour in ternary microemulsion systems formed with non-ionic surfactants. (a) Illustration of the section through the phase prism at equal water and oil content. (b) Schematic phase diagram plotted as temperature versus surfactant concentration C_s . T_L and T_U are the lower and upper temperatures, respectively, of the phase equilibrium W+M+O. T^* is the temperature at which the three-phase triangle is an isosceles, i.e., when the middle-phase microemulsion contains equal amounts of water and oil. This condition is also termed 'balanced'. C_s^* is the surfactant concentration in the middle-phase microemulsion at balanced conditions. 'Lam' denotes a lamellar liquid crystalline phase. After Olsson and Wennerström [68].

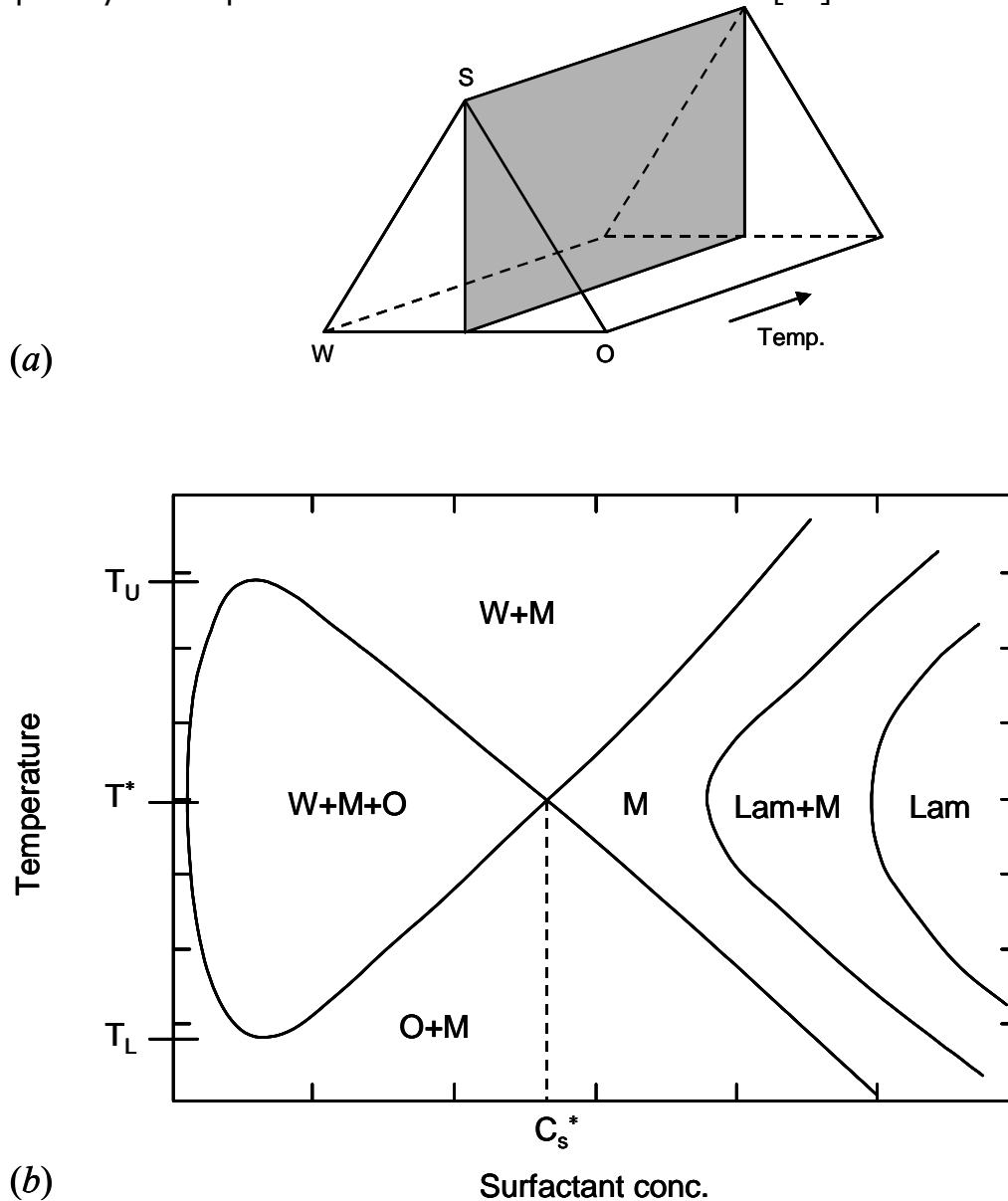


Figure 3.10 Binary phase behaviour in ternary microemulsion systems formed with non-ionic surfactants. (a) Illustration of a section at constant surfactant concentration through the phase prism. (b) Schematic phase diagram, plotted as temperature versus volume fraction of oil, ϕ_o , at constant surfactant concentration. Also shown are various microstructures found in different regions of the microemulsion phase, M. At higher temperatures the liquid phase is in equilibrium with excess water (M+W), and at lower temperatures with excess oil (M+O). At intermediate temperatures a lamellar phase is stable at higher water contents and higher oil contents, respectively. After Olsson and Wennerström [68].

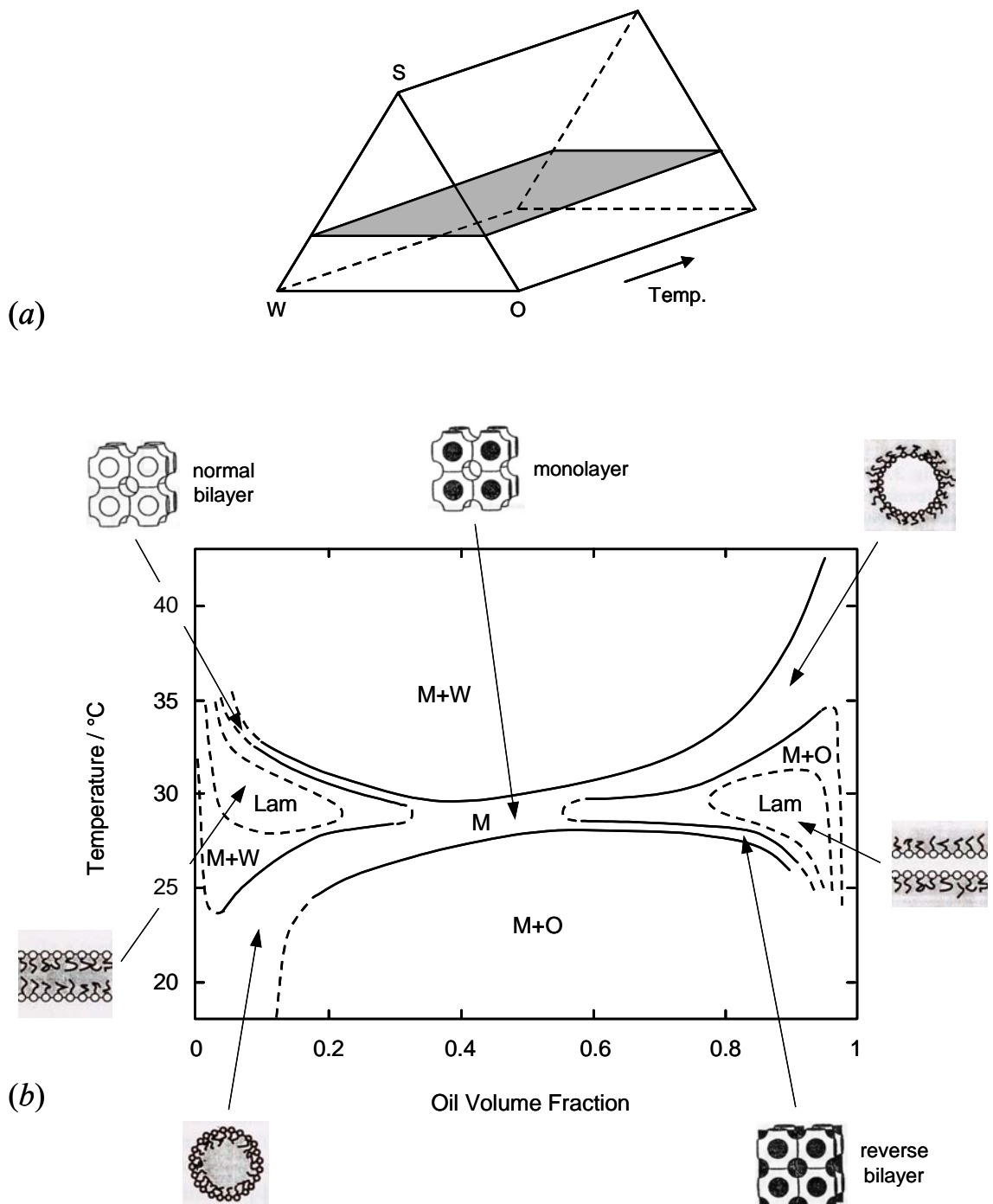
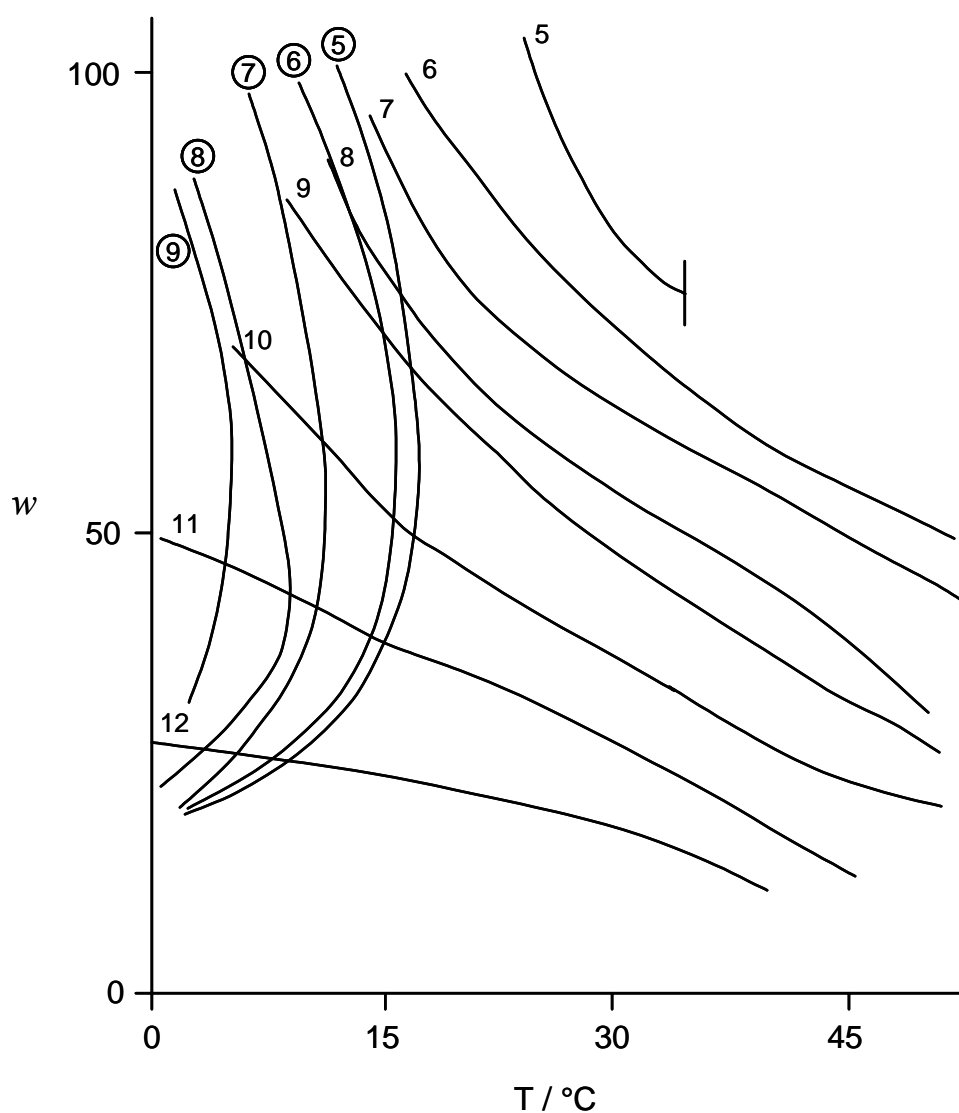


Figure 3.11 Pseudo-binary phase diagram in ternary microemulsion systems formed with the anionic surfactant Aerosol-OT (AOT) in various straight-chain alkane solvents. The water-to-surfactant molar ratio, w , is plotted versus temperature at constant surfactant concentration and pressure. Alkane carbon numbers are indicated; ringed numbers correspond to the lower temperature (solubilisation) boundary, T_L , and un-ringed numbers to the upper temperature (haze) boundary, T_U . The single phase microemulsion region is located between T_L and T_U . Below T_L the system consists of a microemulsion phase in equilibrium with excess water (WII type), and above T_U the single microemulsion phase separates into a surfactant-rich phase and an oil phase. After Fletcher *et al.* [16].



REFERENCES

1. Danielsson, I.; Lindman, B. *Colloids Surf. A* **1981**, *3*, 391.
2. Sjöblom, J.; Lindberg, R.; Friberg, S. E. *Adv. Colloid Interface Sci.* **1996**, *125*.
3. Schulman, J. H.; Stoeckenius, W.; Prince, M. *J. Phys. Chem.* **1959**, *63*, 1677.
4. Shinoda, K.; Friberg, S. *Adv. Colloid Interface Sci.* **1975**, *4*, 281.
5. Adamson, A. W. *J. Colloid Interface Sci.* **1969**, *29*, 261.3.
6. Friberg, S. E.; Mandell, L.; Larsson, M. *J. Colloid Interface Sci.* **1969**, *29*, 155.
7. Shah, D. O., Ed. *Surface Phenomena in Enhanced Recovery* Plenum Press, 1981, New York.
8. Overbeek, J. Th. G. *Faraday Discuss. Chem. Soc.* **1978**, *65*, 7.
9. Tadros, Th. F.; Vincent, B. in *Encyclopaedia of Emulsion Technology* Becher, P. Ed., Vol. 1, Marcel Dekker, 1980, New York.
10. Kunieda, H.; Shinoda, K. *J. Colloid Interface Sci.* **1980**, *75*, 601.
11. Chen, S. J.; Evans, F. D.; Ninham, B. W. *J. Phys. Chem.* **1984**, *88*, 1631.
12. Kahlweit, M.; Strey, R.; Busse, G. *J. Phys. Chem.* **1990**, *94*, 3881.
13. Hunter, R. J. *Introduction to Modern Colloid Science* Oxford University Press, 1994, Oxford.
14. Lekkerkerker, H. N. W.; Kegel, W. K.; Overbeek, J. Th. G. *Ber. Bunsenges Phys. Chem.* **1996**, *100*, 206.
15. Ruckenstein, E.; Chi, J. C. *J. Chem. Soc. Faraday Trans.* **1975**, *71*, 1690.
16. Fletcher, P. D. I.; Howe, A. M.; Robinson, B. H. *J. Chem. Soc. Faraday Trans. 1* **1987**, *83*, 985.
17. Fletcher, P. D. I.; Clarke, S.; Ye, X. *Langmuir* **1990**, *6*, 1301.
18. Biais, J.; Bothorel, P.; Clin, B.; Lalanne, P. *J. Colloid Interface Sci.* **1981**, *80*, 136.
19. Friberg, S.; Mandell, L.; Larson, M. *J. Colloid Interface Sci.* **1969**, *29*, 155.
20. Fletcher, P. D. I.; Horsup, D. I. *J. Chem. Soc. Faraday Trans. 1* **1992**, *88*, 855.

-
21. Winsor, P. A. *Trans. Faraday Soc.* **1948**, *44*, 376.
 22. Bellocq, A. M.; Biais, J.; Bothorel, P.; Clin, B.; Fourche, G.; Lalanne, P.; Lemaire, B.; Lemanceau, B.; Roux, D. *Adv. Colloid Interface Sci.* **1984**, *20*, 167.
 23. Bancroft, W. D. *J. Phys. Chem.* **1913**, *17*, 501.
 24. Clowes, G. H. A. *J. Phys. Chem.* **1916**, *20*, 407.
 25. Adamson, A. W. *Physical Chemistry of Surfaces* Interscience, 1960, p 393.
 26. Bourrel, M.; Schechter, R. S. *Microemulsions and Related Systems* Marcel Dekker, 1988, New York.
 27. Israelachvili, J. N.; Mitchell, D. J.; Ninham, B. W. *J. Chem. Soc. Faraday Trans. 2* **1976**, *72*, 1525.
 28. Griffin, W. C. *J. Cosmetics Chemists* **1949**, *1*, 311.
 29. Griffin, W. C. *J. Cosmetics Chemists* **1954**, *5*, 249.
 30. Davies, J. T. *Proc. 2nd Int. Congr. Surface Act.* Vol. 1 Butterworths, 1959, London.
 31. Israelachvili, J. N. *Colloids Surf. A* **1994**, *91*, 1.
 32. Shinoda, K.; Saito, H. *J. Colloid Interface Sci.* **1969**, *34*, 238.
 33. Shinoda, K.; Kunieda, H. in *Encyclopaedia of Emulsion Technology* Becher, P. Ed., Vol. 1, Marcel Dekker, 1983, New York.
 34. Aveyard, R.; Binks, B. P.; Clarke, S.; Mead, J. *J. Chem. Soc. Faraday Trans. 1* **1986**, *82*, 125.
 35. Aveyard, R.; Binks, B. P.; Mead, J. *J. Chem. Soc. Faraday Trans. 1* **1986**, *82*, 1755.
 36. Aveyard, R.; Binks, B. P.; Fletcher, P. D. I. *Langmuir* **1989**, *5*, 1210.
 37. Sottmann, T.; Strey, R. *Ber. Bunsenges Phys. Chem.* **1996**, *100*, 237.
 38. Langevin, D., Ed. *Light Scattering by Liquid Surfaces and Complementary Techniques* Marcel Dekker, 1992, New York.
 39. Hyde, S.; Andersson, K.; Larsson, K.; Blum, Z.; Landh, S.; Ninham, B. W. *The Language of Shape* Elsevier, 1997, Amsterdam.
 40. Eastoe, J.; Dong, J.; Hetherington, K. J.; Steytler, D. C.; Heenan, R. K. *J. Chem. Soc. Faraday Trans.* **1996**, *92*, 65.

-
41. Eastoe, J.; Hetherington, K. J.; Sharpe, D.; Dong, J.; Heenan, R. K.; Steytler, D. C. *Langmuir* **1996**, *12*, 3876.
42. Eastoe, J.; Hetherington, K. J.; Sharpe, D.; Dong, J.; Heenan, R. K.; Steytler, D. C. *Colloids Surf. A* **1997**, *128*, 209.
43. Eastoe, J.; Hetherington, K. J.; Sharpe, D.; Steytler, D. C.; Egelhaaf, S.; Heenan, R. K. *Langmuir* **1997**, *13*, 2490.
44. Bumajdad, A.; Eastoe, J.; Heenan, R. K.; Lu, J. R.; Steytler, D. C.; Egelhaaf, S. *J. Chem. Soc. Faraday Trans.* **1998**, *94*, 2143.
45. Helfrich, W. Z. *Naturforsch.* **1973**, *28c*, 693.
46. Kellay, H.; Binks, B. P.; Hendrikx, Y.; Lee, L. T.; Meunier, J. *Adv. Colloid Interface Sci.* **1994**, *9*, 85.
47. Safran, S. A.; Tlusty, T. *Ber. Bunsenges. Phys. Chem.* **1996**, *100*, 252.
48. Szleifer, I.; Kramer, D.; Ben-Shaul, A.; Gelbart, W. M.; Safran, S. *J. Chem. Phys.* **1990**, *92*, 6800.
49. Winterhalter, M.; Helfrich, W. *J. Phys. Chem.* **1992**, *96*, 327.
50. Gradzielski, M.; Langevin, D.; Farago, B. *Phys. Rev. E* **1996**, *53*, 3900.
51. Safran, S. A. in *'Structure and Dynamics of Strongly Interacting Colloids and Supramolecular Aggregates in Solution'* Vol. 369 of *NATO Advanced Study Institute, Series C: Mathematical and Physical Sciences*, Chen, S. H.; Huang, J. S.; Tartaglia, P. Ed.; Kluwer, Dordrecht, 1992.
52. Meunier, J.; Lee, L. T. *Langmuir* **1991**, *46*, 1855.
53. Kegel, W. K.; Bodnar, I.; Lekkerkerker, H. N. W. *J. Phys. Chem.* **1995**, *99*, 3272.
54. Sicoli, F.; Langevin, D.; Lee, L. T. *J. Chem. Phys.* **1993**, *99*, 4759.
55. De Gennes, P. G.; Taupin, C. *J. Phys. Chem.* **1982**, *86*, 2294.
56. Daillant, J.; Bosio, L.; Benattar, J. J.; Meunier, J. *Europhys. Lett.* **1989**, *8*, 453.
57. Shneider, M. B.; Jenkins, J. T.; Webb, W. W. *Biophys. J.* **1984**, *45*, 891.
58. Engelhardt, H.; Duwe, H. P.; Sackmann, E. *J. Phys. Lett.* **1985**, *46*, 395.
59. Bivas, I.; Hanusse, P.; Botharel, P.; Lalanne, J.; Aguerre-Chariol, O. *J. Physique* **1987**, *48*, 855.
60. Di Meglio, J. M.; Dvolaitzky, M. Taupin, C. *J. Phys. Chem.* **1985**, *89*, 871.

-
61. Farago, B.; Huang, J. S.; Richter, D.; Safran, S. A.; Milner, S. T. *Progr. Colloid Polym. Sci.* **1990**, *81*, 60.
62. Safran, S. A. *J. Chem. Phys.* **1983**, *78*, 2073.
63. Milner, S. T.; Safran, S. A. *Phys. Rev. A* **1987**, *36*, 4371.
64. Eastoe, J.; Sharpe, D.; Heenan, R. K.; Egelhaaf, S. *J. Phys. Chem. B* **1997**, *101*, 944.
65. Gradzielski, M.; Langevin, D. *J. Mol. Struct.* **1996**, *383*, 145.
66. Eastoe, J.; Sharpe, D. *Langmuir* **1997**, *13*, 3289.
67. Rock, P. A. *Chemical Thermodynamics* MacMillan, 1969, London.
68. Olsson, U.; Wennerström, H. *Adv. Colloid Interface Sci.* **1994**, *49*, 113.